

Transient internal and scattered fields from a multi-layered sphere illuminated by a pulsed laser.

L. Meès*, K.F. Ren, G. Gouesbet and G. Gréhan .

LESP, UMR 6614 / CORIA.
CNRS, INSA et Université de Rouen
BP 12
76801 Saint Etienne du Rouvray

Abstract : This paper is devoted to the interaction between pulsed lasers and multi-layered spheres. Internal and scattered fields are described in a rigorous electromagnetic approach, when a 50 fs pulse illuminates a 80 μm diameter particle. Whispering gallery modes generation inside a core-mantled sphere and effects of a refractive index gradient on scattered fields are in particular exhibited.

1. Introduction

Since many years, a strong effort has been devoted to the description of interaction between laser beams and a family of particles with regular shapes (homogeneous sphere, multi-layered sphere, infinite cylinder with circular or elliptical cross section and ellipsoid), leading to a set of theories assembled under the name of generalized Lorenz-Mie theories (GLMTs). Generalized Lorenz-Mie theories present a particular interest for particle size parameter in the range 1 to 1000, where asymptotic approaches (geometrical optics, Rayleigh scattering) cannot be used (at least not always). These theories have been used, in particular, in the field of optical particle characterization, to design measuring instruments and to analyze their responses. Rather than quoting a literature which is now too large, we kindly request the reader to direct himself to a review paper [1], with more than 350 references. Another way of extending the Lorenz-Mie theory is to consider the temporal description of an electromagnetic interaction when the illuminating beam is a pulsed laser instead of a continuous wave. Such works are motivated by recent progresses in pulsed beam generation which open the way to many applications [2]. A few recent papers are devoted to the description of scattered fields [3-4] and internal fields [5] from a homogeneous sphere illuminated by an ultra-short pulse, providing a temporal separation of optical modes, due to the short length of the pulse (about 30 μm for a 100 fs pulse) when compared with the particle diameter (100 μm).

In this paper, we describe the interaction between a multi-layered sphere and a pulsed laser. This configuration is of importance for metrology of refractive index (or temperature) gradients, or to take into account the case of a sphere with a concentric inclusion. The theoretical aspects are recalled in section 2. Section 3 is devoted to numerical predictions of internal fields in a two layered sphere illuminated by a pulse laser, while section 4 describes the temporal behavior of scattered intensity in the far field for a multi-layered sphere with the number of layers as the main parameter.

2. Theoretical background.

A generic formulation extending GLMTs to pulsed illumination is given in ref. [6]. The electromagnetic incident field at a point \mathbf{r} in space is written as

$$X_i(\mathbf{r}, \tau) = X_0 X_i^s(\mathbf{r}) \exp(2i\pi\nu_0\tau) g(\tau) \quad (1)$$

in which X designates either the electric field \mathbf{E} or the magnetic field \mathbf{H} , subscript i designates field components in a coordinate system matching the geometry of the scatterer. $X_i^s(\mathbf{r})$ is called the spatial support of the pulse, ν_0 is the carrier frequency and the real function $g(\tau)$ is the pulse envelope. The variable τ in eq. (1) is a shifted time

* corresponding author :
mees@coria.fr / tel : 33 (0)2 32 95 37 49 / fax : 33 (0)2 32 95 37 94.

$$\tau = t - \frac{z}{c} \quad (2)$$

in which t is the time variable, z the Cartesian coordinate along the propagation axis of the incident beam and c is the speed of light in free space. The beam described in eq. (1) in the space domain can also be described in the frequency domain in which the response of the scatterer is taken into account. Let the Fourier Transform of $g(\tau)$ be $G(\nu)$ in which ν is the frequency conjugated with τ . Let $X_i^{cw}(r, \nu) \exp(2i\pi\nu\tau)$ be the response of the scatterer to a continuous monochromatic illumination $X_0 X_i^s(r) \exp(2i\pi\nu\tau)$. The response $X_i^p(r, t)$ of the scatterer is then written as :

$$X_i^p(r, t) = \overline{F^{-1}}[G(\nu - \nu_0) X_i^{cw}(r, \nu)] \quad (3)$$

where p and cw stand for “particle” and “continuous wave” respectively and $\overline{F^{-1}}$ designates the inverse Fourier transform where the time variable conjugated with ν is t (and not τ).

In this generic formulation, the shape of the particle is arbitrary and “response of the scatterer” stands either for the scattered field, internal field, forces or couples. In this paper, the scattered particle is a multi-layered sphere and the considered response of the scatterer is the internal or the scattered field response computed in the framework of the Generalized Lorenz-Mie theory for multi-layered spheres [7-9].

3. Internal fields in a core-mantled sphere illuminated by a femtosecond pulse.

Let us consider a core-mantled sphere (2 layers) illuminated by a 50 fs pulse (defined at half width of field amplitude). The core diameter of the particle is 40 μm and its refractive index is $n_1 = 1.6 - 10^{-4}i$. The mantle diameter is 80 μm and its refractive index is $n_2 = 1.3 - 10^{-4}i$. The surrounding medium refractive index is $n_0 = 1$. The carrier wave length of the pulse is $\lambda_0 = 0.6 \mu\text{m}$ and its lateral spatial extension is infinite (plane wave). Figures 1 to 7 show the temporal evolution of the internal intensity (in log. scale) in both core and mantle. In these figures, two dashed circles materialize the interfaces (surrounding medium/mantle and core/mantle) and the incident pulse is incoming from the left. Times indicated on each figure are normalized with respect to time 0 corresponding to the arrival of light at the center of the particle without interacting with it (propagation in free space). In figure 1, at time -100 fs the pulse enters the mantle by refraction. The visible curvature of the pulse is due to a more important delay for light at the center of the figure due to a greater optical path in the mantle with refractive index n_1 . At time 0 fs (figure 2), the central part of the pulse enters the core by refraction when the lateral parts continue to propagate in the mantle. A part of the pulse is also reflected at the core/mantle interface in backward direction (noted R in the figure). The central part of the pulse is again visibly delayed in the core with respect to the lateral parts in the mantle, due to light speed difference in both media.

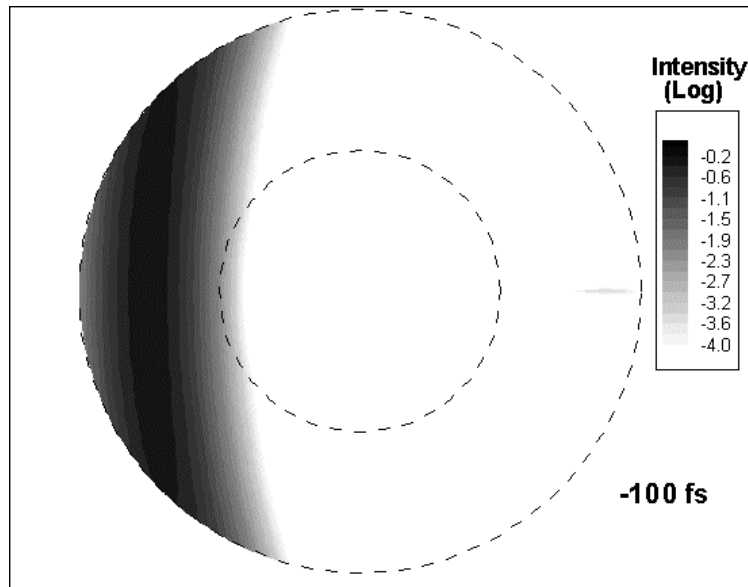


Figure 1 : at -100 fs , the pulse enters the mantle.

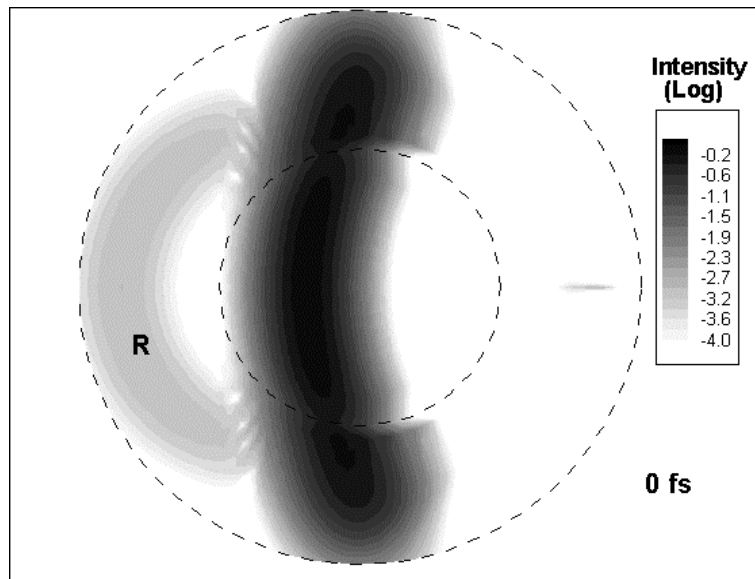


Figure 2: the pulse partially enters the core and is partially reflected at the core/mantle interface.

In figure 3, at time 140 fs , the light is focused in the core, with a focus point behind it, located in the mantle (noted F in the figure). The lateral pulses (A) are also focused in the mantle. The intensity spot noted R in figure 3, corresponds to the light reflected in forward direction at the core/mantle interface. The cutting in reflected light (R) between the backward part in figure 2 and the forward part in figure 3 corresponds to the Brewster angle. Indeed, the polarization is Transverse Magnetic (electric field direction parallel to the computation plane).

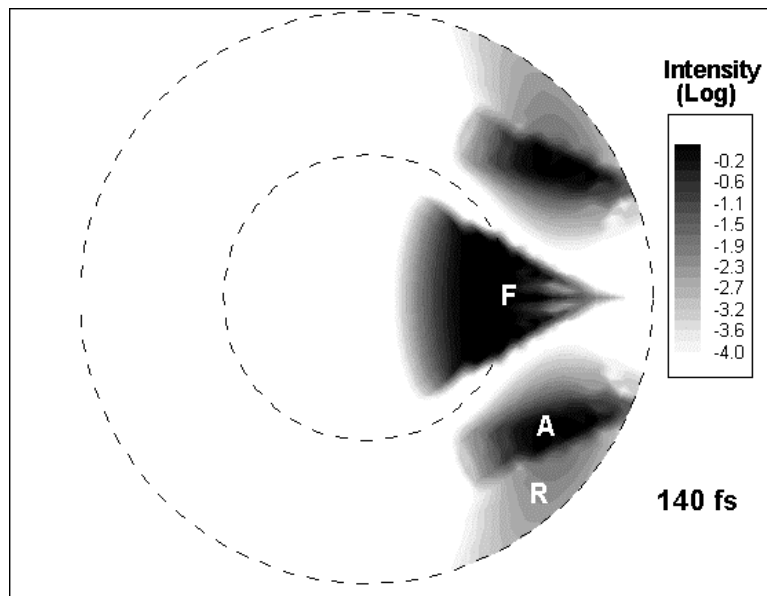


Figure 3 : light is focused in the particle.

In figure 4, at time 240 fs , the light has been internally reflected in the core, in which we distinguish a central part (IR), predictable by geometrical optics and two lateral wave packets, essentially created by diffractive coupling (GM), to be later associated with whispering gallery modes (WGMs) or morphological dependent resonances (MDRs). This behavior has been previously studied in the case of a homogeneous sphere

in ref[5]. At the same time, in the mantle, the two symmetrical spots noted A in figure 3 are now internally reflected at the surrounding medium/mantle interface, creating a focalization hot spot noted F2. 140 fs later, at time 380 fs in figure 5, the internally reflected light at the external interface is also separated in two parts. One central part constituted by "optics rays" which now partially enter the core by refraction (B in figure 5) and are partially reflected at the core/mantle interface (R3). Two symmetrical wave packets noted GM2, similar to the GM spots in figure 4, but in the mantle, are also observed. The spot noted IR in figure 4 joins the core/mantle interface, to be later separate in two parts, one reflected part and one refracted part. Finally, the whispering gallery modes of the core (GM) have been internally reflected, with an energy leakage through the mantle noted L in the figure.

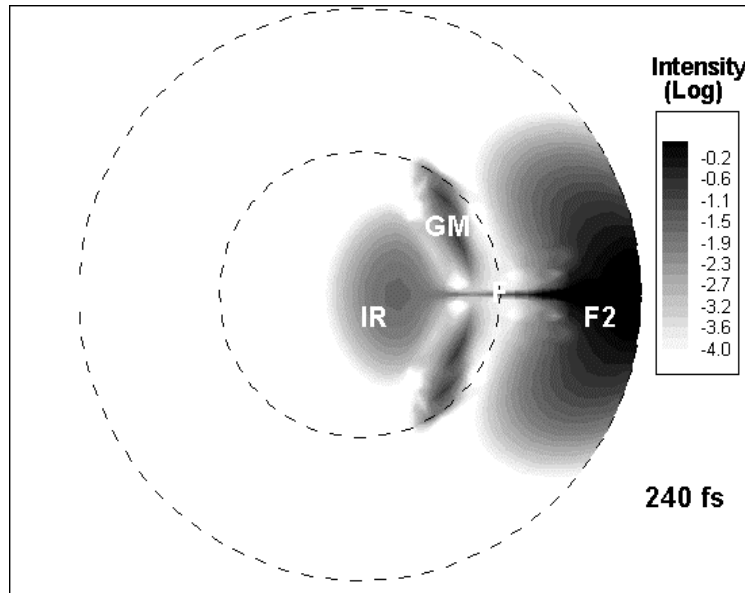


Figure 4 : Whispering gallery modes are initiated in the core.

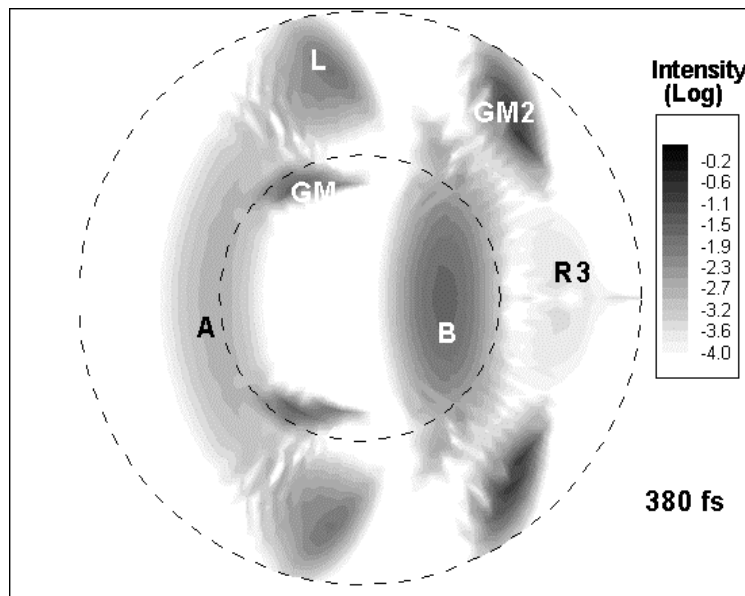


Figure 5 : Internal fields at time 380 fs.

Figure 6 corresponds to time 1060 fs. From this time on, the internal fields are essentially dominated by whispering gallery modes which go on circulating in the particle when lower order modes have vanished, because they travel above the limit angle of refraction and then only leak weakly, by wave effect. A quantification of this leakage in the case of homogeneous spheres is available in reference [5]. WGMs continue

to orbit inside the particle, near the interfaces, during a very long time with respect to the incident pulse duration. See figure 7, in which WGMs are still present 4 ps after the pulse arrival on the particle. This time (4260 fs) also corresponds to a particular situation where the two symmetrical wave packets GM and the two symmetrical wave packets GM2 cross together at the same time.

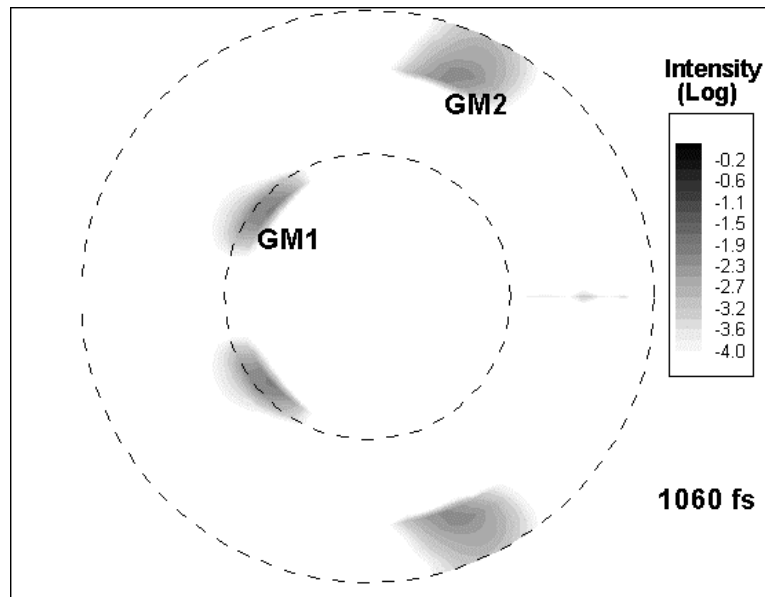


Figure 6 : At time 1060 fs, internal fields are dominated by WGMs.

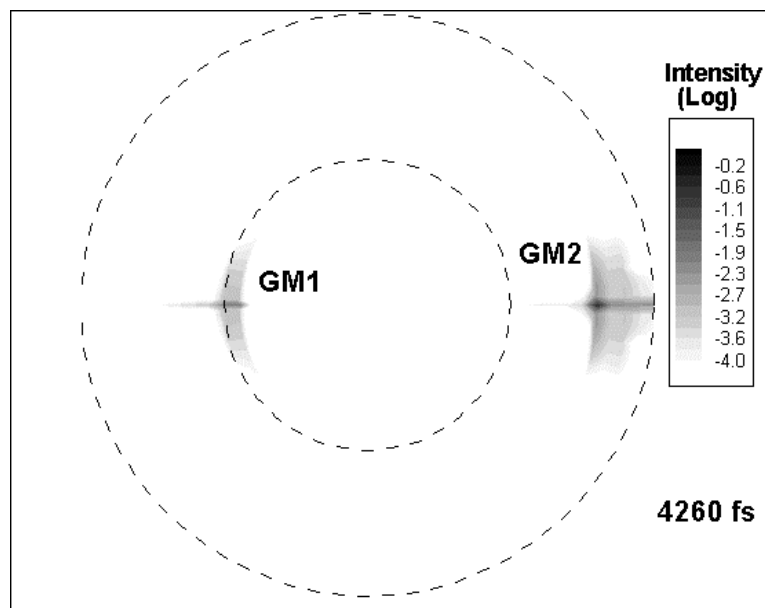


Figure 7 : Internal fields at time 4260 fs. WGMs are still present in the microcavity more than 4 ps after the beginning of the interaction.

4. Scattered intensity in the far field by a multi-layered sphere.

In the previous section we described the internal field in a core-mantled sphere. The temporal separation of optical modes occurring inside the particle is visible because pulse length is shorter than the particle diameter. Indeed, during 50 fs, light travels about 15 μm in free space. The temporal separation is also visible in the far field as mentioned in ref [3] and [4], in the case of homogeneous spheres.

GLMT for multi-layered spheres allows one to consider refractive index gradients, by assuming a large enough number of layers in the particle. Figure 8 displays the scattered intensity in the far field at scattering angle $\theta=45^\circ$ from the forward direction, for a homogeneous sphere (refractive index $n=1.3-10^{-4}i$ and diameter equal to $80 \mu\text{m}$), a 2-layers sphere and a 4-layers sphere. The incident pulse is the same than in section 3. All multi-layered spheres in this section have an external diameter equal to $80 \mu\text{m}$, the refractive index is $n=1.3-10^{-4}i$ for the more external layer and $n=1.6-10^{-4}i$ for the central sphere. Intermediary layers have intermediary diameters and intermediary refractive indices as displayed in table 1, in the case of 4 layers. Note that the 2-layered sphere is the same than in previous section.

Table 1 : definition of the 4-layers sphere.

Layer number	Diameter	Refractive index
1	$20 \mu\text{m}$	$1.6-10^{-4}i$
2	$40 \mu\text{m}$	$1.5-10^{-4}i$
3	$60 \mu\text{m}$	$1.4-10^{-4}i$
4	$80 \mu\text{m}$	$1.3-10^{-4}i$

The scattered intensity in figure 8 takes the form of a succession of peaks, relative to the temporal separation of modes. The first peak labeled A corresponds to the light reflected by the particle (external interface). This optical mode occurs at the shortest time because it corresponds to the shortest optical path. The intensity and temporal location of peak A is unchanged with the number of layers, according to an unchanged relative refractive index between the surrounding medium and the external layer of the particle. When only considering the first curve corresponding to homogeneous sphere, we observe 3 other peaks labeled B, C and D. Peak B corresponds to light refraction through the particle, with a time delay with respect to peak A, corresponding to an extra optical path relative to the travel inside the particle with a refractive index greater than 1. Peaks C and D correspond to the leakage of wave packets described in previous section after 3 and 4 internal reflections respectively. The larger time delays associated with the peaks C and D also correspond to longer paths in the particle. When the particle is a multi-layered sphere, intermediary interfaces produce intermediary peaks in figure 8. See for example the additional peak between A and B in the case of the 2-layers particle, which corresponds to the light refracted at the external interface, reflected at the internal interface (spot labeled R in figure 3 of the previous section) and again refracted at the external interface. In the case of a 4-layers sphere, 3 intermediary peaks occur between A and B. More generally, one can observe the increase of the multiplicity of peaks when the number of layers increases.

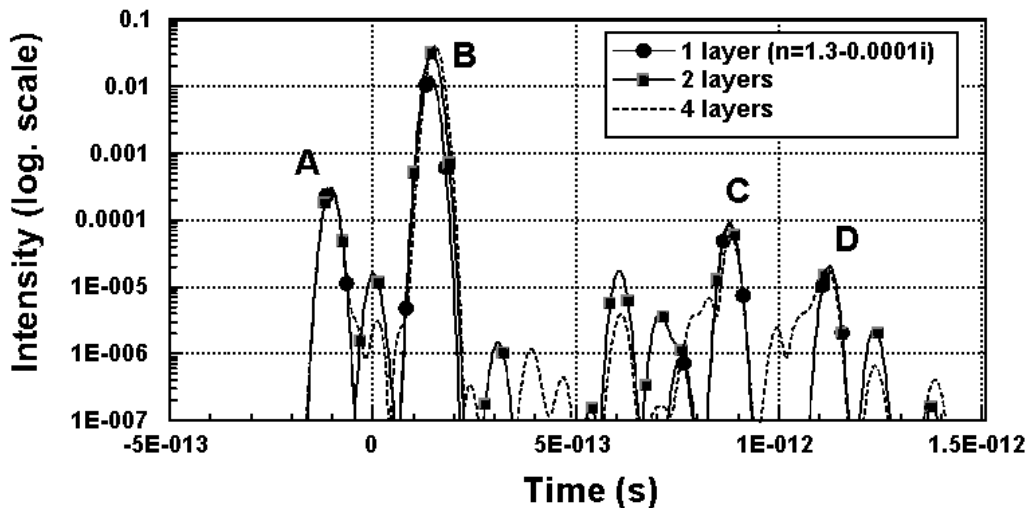


Figure 8 : Scattered intensity at $\theta=45^\circ$ in the far field versus time, for a homogeneous sphere ($n=1.3-10^{-4}i$), a 2-layers sphere, and a 4-layers sphere.

When the number of layers increases much in the particle, we are progressively facing the case of a gradient of refractive index. As a consequence, the intermediary peaks of figure 8 disappear when the number of layers reaches say 128, i.e. results are then unchanged when considering more layers. In figure 9, we compare the scattered intensity by homogeneous spheres with refractive index $n=1.3-10^{-4}i$ and $n=1.6-10^{-4}i$ and a sphere

with a refractive index gradient from $1.6 \cdot 10^{-4}i$ at the center to $n=1.3 \cdot 10^{-4}i$ at the particle surface (128 layers). The peak A remains unchanged as previously justified, but other peaks occur at larger times for a larger refractive index with peak intensity changes. In the case of a refractive gradient, location of peaks is intermediary. However, when considering a homogeneous sphere with an intermediary refractive index $n=1.45 \cdot 10^{-4}i$ (see figure 10), both location and intensity of peaks remain different with respect to the case of particle with gradients. In particular, peaks labeled C and D are strongly affected by the index gradient of the particle.

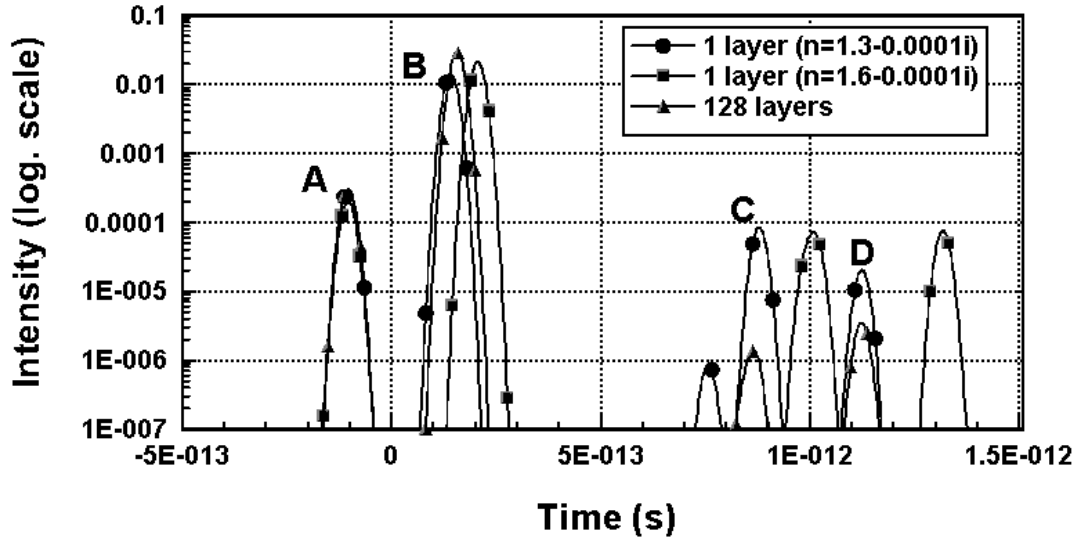


Figure 9 : Scattered intensity at $\theta=45^\circ$ in the far field versus time, for a homogeneous sphere with $n=1.3 \cdot 10^{-4}i$, a homogeneous sphere with $n=1.6 \cdot 10^{-4}i$, and a sphere with refractive index gradient from $1.6 \cdot 10^{-4}i$ at the center to $n=1.3 \cdot 10^{-4}i$ at the particle surface (128 layers).

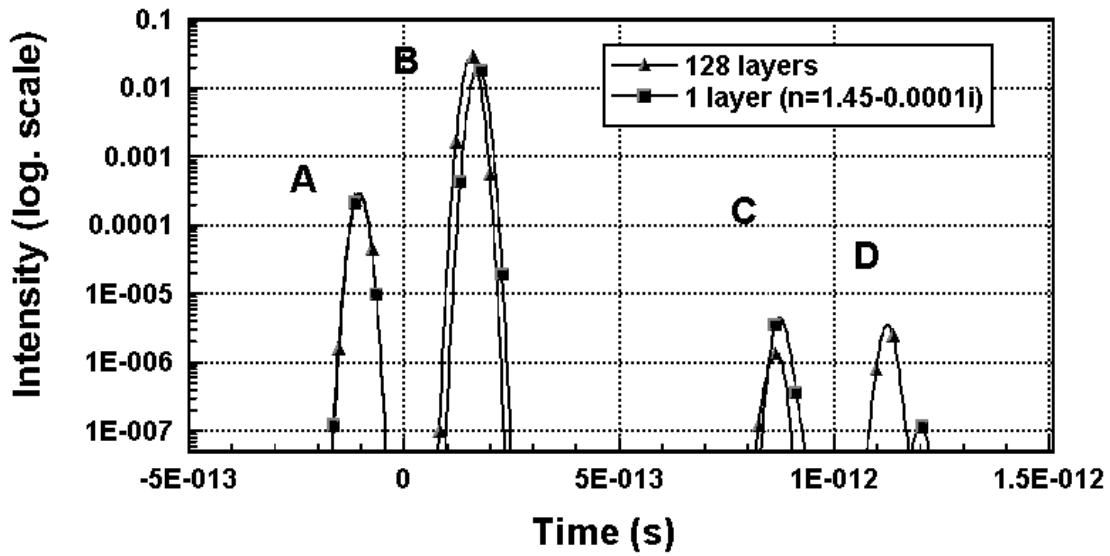


Figure 10 : Scattered intensity at $\theta=45^\circ$ in the far field versus time, for a homogeneous sphere with $n=1.45 \cdot 10^{-4}i$, and a sphere with refractive index gradient from $1.6 \cdot 10^{-4}i$ at the center to $n=1.3 \cdot 10^{-4}i$ at the particle surface (128 layers).

- [1] G. Gouesbet and G. Gréhan (2000). Generalized Lorenz-Mie theories, from past to future. *Atomization and Sprays*, 10 (3-5) 277-333.
- [2] C. Fabre and J.P. Pocholle (1996). *Les lasers et leurs applications scientifiques et médicales* (Les Editions de Physique, Fr)
- [3] L. Méès, G. Gouesbet and G. Gréhan. Time resolved scattering diagrams for a sphere illuminated by plane wave and focused short pulses. *Optics communications* 194 (2001) 59-65.
- [4] L. Méès, G. Gouesbet and G. Gréhan. Scattering of laser pulses (plane wave and Gaussian beam) by spheres. *Applied Optics* Vol. 40, No 15, pages 2546-2550, 2001.
- [5] L. Méès, G. Gouesbet and G. Gréhan. Interaction between femtosecond pulses and a spherical microcavity : internal fields. *Optics communications* 199 (2001) 33-38.
- [6] G. Gouesbet and G. Gréhan, Generic formulation of a generalized Lorenz-Mie theory for a particle illuminated by laser pulses, *Part. Part. Syst. Character.* 17, 5-6, 213-224, 2000
- [7] F. Onofri, G. Gréhan and G. Gouesbet. Electromagnetic scattering from a multi-layered sphere located in an arbitrary beam. *Applied Optics*, 34 (30) : 7113-7124, 1993.
- [8] Z. S. Wu, L. X. Guo, K. F. Ren, G. Gouesbet and G. Gréhan. Improved algorithm for electromagnetic scattering of plane waves and shaped beams by multilayered spheres', *Applied Optics* 36 (21) : 5188-5198, 1997.
- [9] K. F. Ren, Loïc Méès, G. Gréhan and G. Gouesbet. Internal fields of a multilayered sphere illuminated by a Gaussian beam. Under preparation, 2002.